Copyright Warning & Restrictions

The copyright law of the United States (Title 17, United States Code) governs the making of photocopies or other reproductions of copyrighted material.

Under certain conditions specified in the law, libraries and archives are authorized to furnish a photocopy or other reproduction. One of these specified conditions is that the photocopy or reproduction is not to be "used for any purpose other than private study, scholarship, or research." If a, user makes a request for, or later uses, a photocopy or reproduction for purposes in excess of "fair use" that user may be liable for copyright infringement,

This institution reserves the right to refuse to accept a copying order if, in its judgment, fulfillment of the order would involve violation of copyright law.

Please Note: The author retains the copyright while the New Jersey Institute of Technology reserves the right to distribute this thesis or dissertation

Printing note: If you do not wish to print this page, then select "Pages from: first page # to: last page #" on the print dialog screen

ABSTRACT

Wear and Friction of Titanium Nitride on Ultra High Molecular Weight Polyethylene Under Oscillating Motion for Evaluation of Use in Articulating Orthopedic Applications

by
David Scott Jacobson

Materials are a factor in the performance of articulating orthopedic implants. An oscillating tribometer is utilized to investigate mechanisms of wear and friction of TiN (titanium nitride) coated on Ti-6Al-4V (titanium) alloy against UHMWPe (ultra high molecular weight polyethylene). Three thicknesses of TiN coating (1.76 μm, 4.15 μm, and 10.5 μm) are used to evaluate the performance of each in UHMWPe wear reduction and coating integrity. An uncoated Co–Cr (cobalt chromium) coupon is used against UHMWPe pins for control purposes. Oscillations are carried out to 10 million cycles to discover and evaluate short- and long-term wear mechanisms. Mass differentials and torque are recorded for each test at specific intervals in order to establish wear volumes and rates of the UHMWPe, and coefficients of friction. Profilometries and polarized light photomicrography are performed at test conclusion to observe any alteration in physical condition which occurred during each test. Analysis of the results reveals the benefit of reduced wear from a TiN/Ti-6Al-4V coating-substrate system coupled with UHMWPe. Use of TiN/Ti-6Al-4V enables a reduction in abrasive wear and a reduction and delay in the onset of adhesive wear and associated UHMWPe transfer films. UHMWPe wear decreases with thinner TiN coatings, realizing up to two-thirds reduction in wear over a Co–Cr-UHMWPe system. Even with a rougher surface a TiN-UHMWPe system (pre-test R_a = 0.07–0.11) benefits with a minimum of one-third reduction in UHMWPe wear over the smoother Co–Cr-UHMWPe system (pre-test R_a = 0.03).

WEAR AND FRICTION OF TITANIUM NITRIDE ON ULTRA HIGH MOLECULAR WEIGHT POLYETHYLENE UNDER OSCILLATING MOTION FOR EVALUATION OF USE IN ARTICULATING ORTHOPEDIC APLICATIONS

by
David Scott Jacobson

A Thesis
Submitted to the Faculty of
New Jersey Institute of Technology
in Partial Fulfillment of the Requirements for the Degree of
Master of Science in Biomedical Engineering
May 1992

APPROVAL PAGE

Wear and Friction of Titanium Nitride on Ultra High Molecular Weight Polyethylene Under Oscillating Motion for Evaluation of Use in Articulating Orthopedic Applications

by
David Scott Jacobson

Dr. Michael J. Pappas, Thesis Advisor
Research Professor of Mechanical Engineering, NJIT

Dr. David S. Kristol, Committee Member
Director of Biomedical Engineering Program, NJIT

Dr. Clarence Mayott, Committee Member
Associate Professor of Mechanical Engineering, NJIT

BIOGRAPHICAL SKETCH

Author: David Scott Jacobson

Degree: Master of Science in Biomedical Engineering

Date: May, 1992

Undergraduate and Graduate Education:

- Master of Science in Biomedical Engineering,
  New Jersey Institute of Technology, Newark, NJ, 1992
- Bachelor of Arts in Psychology
  University of Michigan, Ann Arbor, MI, 1989

Major: Biomedical Engineering

Presentations and Publications:

Jacobson, David. "Wear and Friction of Titanium Nitride on Ultra High Molecular Weight Polyethylene in Articulating Orthopedic Applications." Presented in Kingston, Rhode Island, March, 1992, at the 18th IEEE Northeast Biomedical Engineering Conference.

Jacobson, David. "Wear and Friction of Titanium Nitride on Ultra High Molecular Weight Polyethylene in Articulating Orthopedic Applications." Presented in Newark, NJ, April, 1992, at Mini-Tec 1992.

ACKNOWLEDGEMENT

I wish to express my sincere gratitude to my supervisor, Professor Michael J. Pappas, for his guidance throughout this research.

A very special thank you to Professors David Kristol and Clarence Mayott for serving as committee members. Furthermore, added thanks are due to Professor Kristol for all the support and encouragement he has offered over the past two years.

Unending appreciation is extended to George Makris for his knowledge, friendship and moral support during this research.

I am grateful to Ceiba-Geigy Corporation for inital funding of this research and to Biomedical Engineering Trust for providing further and continued funding, equipment, and facilities for this project.

I would like to extend recognition to Multi-Arc Scientific for use of equipment and help in material preparation.

And finally, a special thanks to the employees of Endotec, Inc. for helping to make this work an enjoyable experience.

TABLE OF CONTENTS

Page

LIST OF TABLES

Table **Page**

LIST OF FIGURES

Figure **Page**

LIST OF FIGURES (continued)

Figure **Page**

CHAPTER 1
INTRODUCTION

Decisions regarding material selection are some of the most important when considering articulating orthopedic implants. Articulating orthopedic implants replace damaged, diseased, or worn joints. There are three properties that must be addressed of each material: mechanical, physical and chemical. The first two of these include those properties which control the functional characteristics of most implants. It is the choice of the material, based on properties necessitated by the application and the characteristics of that material, that determines the functional suitability of the implant. The chemical properties of the material, shown by the reactions exhibited between it and the environment of the body, control the ability of the implant to maintain its function throughout its period of use.

During the period between 1920 to 1950, several developments took place in the field of orthopedic implant surgery which are the basis of some of today's more modern techniques. In the early 1920's there was still no one metal or alloy that could be regarded as a functionally useful implant material. Both gold and silver, although relatively inert and reasonably well tolerated by the tissues, were too soft and weak for most applications and could only be used effectively as plating on other metals or as sutures or wires. Copper was stronger but not well tolerated by the body and copper alloys suffered the same disadvantage. Lead was both too soft and too toxic. Aluminum and some of its alloys provided some hope, but again, biocompatibility was not adequate, with the metal disintegrating in the body. Magnesium met the same fate when it was used. Iron and steel were the most commonly used. The majority of these ferrous materials rusted over time in the body causing tissue discoloration, and most possessed limitations in their mechanical properties.

The introduction of stainless steels had appeared to solve some of the mechanical

problems associated with implant materials. 18-8 stainless steel was introduced into the surgical world in 1926 as a new corrosion resistant material. However this nominally corrosion-resistant material was found to corrode frequently and deleteriously in the environment of the body. A modified stainless steel, 18-8-S Mo, which contained 2 to 4 percent of molybdenum, conferred greater resistance to corrosion in saline solutions. Nevertheless, 18-8-S Mo did not offer the intercorporeal corrosion resistance that is desired for implants and the biocompatibility for resulting implant wear particles was poor.

Venable and Stuck looked further for metals and alloys that did not corrode in the body and did not cause any irritation of the tissues. They used an alloy of cobalt, chromium and molybdenum, stellite (Co–Cr). This experimentation was done in 1936, seven years after stellite had been developed and a few years after it had been used as a dental alloy. Venable and Stuck found that it was inert in the body, producing far less destruction of the bone around the implanted materials.

In 1938 the first total hip replacement was performed. Wiles inserted six such implants and they had some success. However ten years later a follow-up study revealed adverse reaction of the bone to the prosthesis. The Judet brothers developed the first femoral hip prosthesis designed on 'mechanical principles.' It was also the first implant to use polymethylmethacrylate (PMMA) in a major component of its construction. Severe criticisms were, nonetheless, levelled at the Judet prosthesis. They were basically due to the underestimation of the mechanical forces involved in the hip joint and the unwarranted faith in the mechanical properties of PMMA. The results at first were very positive, but the material itself had proved unsuitable and ultimately fragmentation, erosion, and the flaking off of small particles commonly occurred. In addition, fixation of the stem of the prosthesis in the femoral neck was often inadequate, leading to displacement or fracture of the stem [1, 2].

The titanium-aluminum-vanadium alloy Ti-6Al-4V (Table 1) has many very

desirable properties for an implant material. Introduced for implant use in 1951 this titanium alloy is the most inert metal yet used for implant fabrication [2, 3]. In comparison with other implantable metals, titanium alloys are the most biocompatible, the lightest, the strongest, and the most corrosion and fatigue resistant. Its modulus of elasticity is roughly one-half of the others and therefore closer to bone [2, 3]. However, it is not scratch resistant. Therefore, its use in articulating implants has been for the most part discontinued.

TABLE 1: Ti-6Al-4V ELI* (Elements by Weight Percent)

Al	V	Fe	C	N	O	H	Ti
6	4	<0.25	<0.08	<0.05	<0.13	<0.012	Balance

*Ti alloy 6Al-4V ELI according to ASTM F 136-84

Using Co–Cr alloy Moore (1959) and Thompson (1954) introduced their femoral head replacement prostheses. The prostheses however wore through the bone in the acetabulum and moved through the pelvis under the influence of the applied loads [1]. Modifications continued through many designs until Charnley revolutionized prosthesis design. For an unlubricated bearing, a metal alloy or ceramic coupled with a plastic has the lowest coefficient of friction, the lowest wear rate, and acceptable compatibility with the body. It was on this basis that the first metal-plastic total hip replacement was introduced by Charnley in 1959. It was not a success, however, because the plastic acetabular cup was polytetraflouroethylene (PTFE), or Teflon, and the wear of this material was considerable. Further, wear debris of PTFE, unlike the bulk material, is highly reactive. Charnley updated his design and replaced the PTFE first with high density polyethylene and then with ultra high molecular weight polyethylene (UHMWPe) achieving much better results [4, 5]. Since Charnley demonstrated its properties as a bearing material in combination with metal surfaces [6], the metal on UHMWPe combination has become universal in joint replacement implants for the hip and knee.

The most widely used implant material today is a cobalt chromium (Co–Cr) alloy.

This alloy has been used for implants primarily because of its resistance to scratching [5]. However, there have been problems. Cobalt chromium alloys have major disadvantages in their fatigue strength and modulus of elasticity when compared to cortical bone. Evidence also implicates elements of the Co–Cr alloy as carcinogenic [7].

During a tribological analysis of retrieved Charnley hip prostheses Isaac [8] noted that the "level of damage to the acetabular cup was surprising." Charnley UHMWPe acetabular cups articulate with a Co–Cr femoral counterpart. The mean penetration rate, a measure of the penetration of the metal femoral head into the UHMWPe of the acetabular cup, was 0.21 mm per year with a maximum up to 6 mm per year. High penetration rates preclude a long implant life. It is therefore likely that reducing the rate of wear would improve the performance of the artificial hip joint. The wear in this study can in part be attributed to particles of PMMA as all the implants in the study used cement for fixation. Nevertheless, it can be theorized that while the rates would not be as high, problems with wear have similar consequence with cementless implants. Of the 100 retrieved hips analyzed by Isaac, 92 failed due to problems relating to wear and associated loosening of the acetabular cup. Wroblewski and Rimnac [9, 10] have also reported the strong relationship between wear in acetabular cups and acetabular socket implant loosening. Furthermore, the potential for bone resorption and implant loosening as a result of fibrous tissue aggravated by polymeric wear debris has become well documented in both knee and hip implants [11, 12, 13].

Switching to an implant material which induces less wear in the UHMWPe may result in a reduction in clinical wear rates. High wear rates limit the service life of a joint and it is probable that changes reducing the these rates would improve the performance of a joint.

Composites have been explored. While having a modulus approaching that of bone and high strength, carbon/resin composites have been rejected because of their toxicity. Carbon/carbon composites were also investigated because of their advantages:

biocompatibility, a density close to cortical bone, heterogeneous structure, elasticity approaching that of cortical bone, and chemical inertia. However, the material fails in the realm of hardness and wear resistance [14]. Titanium alloys have the benefits, as stated before, of light weight and high fatigue strength—important properties in a long-life device—but are poor in the area of wear control unless treated [14].

The recent application of thin ceramic coatings seems to have opened up new perspectives on the use of titanium alloys in articulating orthopedic implants. In 1988 a patent was granted for a method of applying a thin layer of titanium nitride (TiN) onto orthopedic implants [14]. Thin coatings must meet specific criteria for the desired application (Figure 1). This coating method was hoped to resolve biocompatibility and/or mechanical interface problems which complicated the use of previous implant materials. TiN coatings are very hard and wear resistant [14, 15]. The coating thickness is very small, on the order of microns, maintaining the dimensional stability of the part to be coated [16]. Thin layers of TiN tend to assume the deformation and fatigue strength properties of the substrate [17]. Further enhancing biocompatibility, the TiN coating itself is biocompatible and the TiN coating eliminates metallic wear debris caused by metal-UHMWPe articulation [14, 15, 19]. TiN also increases corrosion resistance and reportedly reduces the coefficient of friction of coated metal surfaces against UHMWPe [19]. Properties of TiN are given in Table 2. Subsequent approval by the FDA, as evident by the sale of TiN-coated implants, has further made it an attractive option.

Initial attempts at a TiN hard coating were tried via the method of Chemical Vapor Deposition. With this technique TiN is produced chemically from gaseous components at high temperatures by catalytic influence of the substrate surface [20]. However, the high temperatures used (800 to 1100 °C) distort the high tolerance designs of orthopedic implants and can also cause a loss of substrate hardness.

The method that was then explored, and is currently being used, was Physical Vapor Deposition (PVD). The low temperatures, in the range of 300 to 450 °C, do not

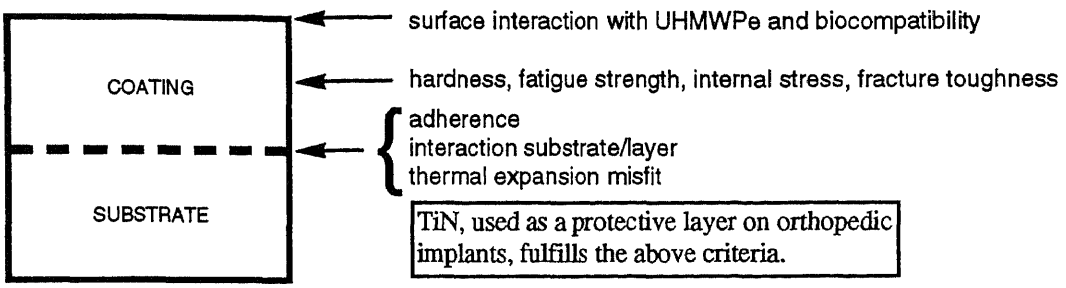

FIGURE 1: Important Criteria for Coating Selection [18]

TABLE 2: Properties of TiN Coating [18]

Density (g/cm³)	5.40	*E* Modulus (kN/mm²)	590
Melting point (°C)	2950	Specific electrical resistivity (μΩ cm)	25
Hardness (HV)	2100	Thermal expansion coefficient (10^{-6} K^{-1})	9.4
Color	Golden yellow		

cause a loss of hardening or distortion to the materials being coated. Describing the PVD method would be incomplete without first stressing the importance of pre-coating procedures. After fabrication the parts are polished. To obtain good adhesion with the coating, the surface must be free from contaminants to allow ionic bonding. Therefore, parts are freon degreased, ultrasonically cleaned, water rinsed, and sent through a freon dry sequence. Parts are placed onto a fixture and moved into the coating chamber. Before applying the hard coating, though, this method first applies a high energy ion beam in a conditioning stage which serves to further purge the surface of impurities and thin oxide films. The added cleansing action of this process insures good adhesion of the coating to the substrate. Subsequently, the chamber is filled with a nitrogen atmosphere. A bias voltage is created between the implants (*anodes*) and a piece of solid titanium (*cathode*), and the cathode is vaporized (Figure 2).

The vapor generation phase of the PVD process can be approached in a few ways: evaporation from a crucible, sputtering, and evaporation using a vacuum arc [20]. Evaporation from a crucible uses an electron beam in a triode arrangement or as a low voltage arc evaporator. The plasma over the crucible is generated by an electron beam and the vapor is ionized in a second working stage. Since the material to be evaporated is present in a molten condition, the evaporators must be installed at the bottom of the vacuum chamber [20]. Sputtering is a method by which a solid metal cathode is bombarded with high energy gas ions causing detachment of the atoms at the cathode surface. A carrier gas such as argon is required for these bombarding ions, and ionization takes place when the vapor particles pass through the glow discharge plasma [20]. With arc evaporation, the metal is simultaneously evaporated at microscopically small areas and the vapor particles are ionized and accelerated all in one working stage.

The arc PVD process gives the highest degree of ionization, the highest average ion energy and more than adequate ion current density at the substrate for every application. Arc evaporation also gives the most uniform coating because evaporators

can be placed around the perimeter of the chamber [20]. By concentrating an arc on the cathode, titanium is eroded into three forms: ions (80 percent), uncharged metal vapor and metal droplets [20]. Minimizing droplets is important because droplets can cause defects to the surface finish which can lead to quality and assurance rejection. The coating is applied by bombarding the implant surface with titanium ions which combine in the nitrogen rich atmosphere to form the TiN coating on the implant. During coating the bias voltage is reduced into the range of -100 to -150 V. The ions have enough energy to remove any loosely adhering coating over the duration of the coating process. This ion beam ensures coating compression and an optimum amount of nitrogen included in the ceramic [20]. Coating thickness is altered by fluctuating the evaporator current and the time of coating. Primarily, the evaporator current and coating time have linear relationships with the coating thickness. However, this still appears to be an inexact science as the same coating parameters may yield slightly varying coating thicknesses. After coating, it is not unusual for the TiN surface to be of a roughness not approaching implant quality even when using very smooth substrate material. The TiN surface, however, can be polished with diamond pastes to achieve excellent results ($R_a \leq 0.05$) allowing uncompromised implant use [19].

The present pin-on-disk test is a tribological study of TiN on UHMWPe. Friction, the force acting against the relative sliding of surfaces, and wear, the loss of material from at least one of those surfaces, have been the two main areas of investigation in tribo systems. Friction is the resistance to motion arising at the interface of two surfaces attempting to slide over the other. Wear is the removal or relocation of material arising from the contact of two surfaces. *Abrasive wear* occurs when a rough, hard surface slides over a much softer surface and ploughs a series of grooves in it. The material from the grooves is displaced in the form of wear particles. *Surface fatigue* wear occurs under repeated loading and sliding cycles which may result in the formation of surface cracks and the eventual break-up of the surface. *Adhesive wear* is the

consequence of two solids sliding over each other such that fragments are pulled off one surface and adhere to the other. These fragments may then be transferred from one surface to the other during later cycles, or possibly emitted as loose particles. When a force tangential to the interface is applied, there are several possible pathways for the shear to take place. It may occur along the interface in which case nothing is gained or lost from either material. If, however, the force necessary to shear the interface is larger than to shear one of the materials itself, the shear may occur with the material, and a transferred wear particle is produced [22]. An evaluation of wear and frictional forces at the interface of TiN coating and UHMWPe will allow a more educated use in articulating orthopedic implants.

In the 1940's, Bowden and Tabor pioneered much of the basics of tribology with their studies on the friction and lubrication of solids [22]. A great deal of work has been done since studying tribological mechanisms as they relate to orthopedic implants. There is, however, very limited information regarding the evaluation of coating-substrate systems (i.e TiN coated onto a Ti-6Al-4V substrate) and also the wear performance of the interaction of such coatings with UHMWPe [19, 25, 28].

Even fewer tests have utilized an oscillating tribometer to simulate the repetitive motion associated with body movements such as standing from a sitting position, walking, etc [27]. In the hip, articulation is of a sliding nature and it is such sliding motion that is reproduced in the present study. Furthermore, as body joint motion is oscillatory, wearing upon a surface repeatedly for millions of cycles, evaluations which used non-oscillating pin-on-disk tribometers [19] do not account for the change in direction and change in velocity present under physiological conditions and in oscillating tests. Such changes prevent boundary lubrication effects over the sliding distance and hydrodynamic lubrication effects at the end of the wear tracks. A more severe and realistic test is performed with oscillation.

Martinella has utilized the oscillating wear-tester format [27], but not with both

UHMWPe and TiN. He did, however, conclude that his findings "validate the [tribometer] as a source of data suitable to evaluate different materials in simulative conditions and to predict *in vivo* wear behaviour of UHMWPe-metal prosthesis."

Previous research has also focused on the metal or coating/substrate system [19, 23, 24, 25, 26] rather than giving a weighted concern to the wear effected upon the UHMWPe bearing. Tests which have measured the adhesive forces of the TiN coating to a Ti-6Al-4V substrate show that when properly applied its adhesion properties are excellent [19, 23, 24, 25, 26]. Evaluation of the UHMWPe is important because failure of the bearing portion of an implant will necessitate revisional surgery for its replacement.

Past experience has shown that Co–Cr, the current standard material of articulating implants, is not sufficient. The alloy is not ideal in many aspects: a fatigue strength that is too low, a modulus that is too high, a weight that is too high, and carcinogenic elements. Co–Cr's greatest benefit is its scratch resistance—but even this is not without want for improvement; clinical results reveal many scratches on retrieved Co–Cr implants [8].

The desire for an articulating implant system that will excel where the Co–Cr-UHMWPe system has failed leads to alternative materials. Titanium alloys are superior in all aspects to Co–Cr, with the exception of scratch resistance. The application of TiN onto a Ti-6Al-4V substrate may offer the scratch resistance and superior wear characteristics desired via the coating as well as unparalleled mechanical properties and inertness for a metal substrate. The prospect of superior performance of TiN/Ti-6Al-4V on UHMWPe over Co–Cr on UHMWPe is of great importance.

The current study is not a simulator study. Simulator studies use actual implants, but have been sparingly used because of the cost and design factors that complicate their use. However, data from simulator studies can be extremely valuable. In a simulator study it has been shown that TiN can reduce the UHMWPe wear by two-thirds over

Co–Cr's performance [28] and can foster a threefold decrease in wear over Ti-6Al-4V implants [19]. Nevertheless, additional data that directly relate to the total wear of both components of an articulating implant system and suggestions on how to minimize such wear is needed.

CHAPTER 2
OBJECTIVE

The pin-on-disk test that has been constructed for this evaluation was designed to quickly and reliably identify parameters for TiN coatings on Ti-6Al-4V in a cost-effective manner for which more expensive and time intensive joint simulator testing can then be justified. Furthermore, this type of testing enables relationships to be formed in a practical manner between wear and materials and their finishes.

With consideration to past work this study seeks to evaluate both systems and make conclusions as to their performance. The properties of various coating thicknesses and roughnesses of TiN on an orthopedic implant's tribo-system has not been explored. A better understanding of how TiN interacts with the bearing surface UHMWPe will allow an insight into what and if any improvements in wear are available using TiN/Ti-6Al-4V and how any future improvements may be made as a consequence of variations of the coating and finishing parameters.

CHAPTER 3
METHODOLOGY

The purpose of this study is to evaluate the wear properties of TiN/Ti-6Al-4V on UHMWPe under oscillating motion and constant load and compare results to Co–Cr oscillating on UHMWPe under the same conditions.

Metal coupons are machined from either Ti-6Al-4V ELI or Co–Cr rod stock. The Ti-6Al-4V ELI coupons are sintered, put through polishing and cleaning procedures and then coated with UltraCoat™, a TiN coating. The TiN is applied to three coupons in thicknesses of 1.76 μm, 4.15 μm, and 10.5 μm. Coating thickness is established using a ball-and-crater test on a not-to-be-used portion of the coupon surface. It is commercially applied using the arc evaporation method of the PVD process, the details of which are similar to those described in the introduction of this paper. An uncoated Co–Cr coupon is used as a control. The 4.15 μm TiN-coated Ti-6Al-4V coupon, the 10.5 μm TiN-coated Ti-6Al-4V coupon, and the Co–Cr coupon are diamond paste lapped prior to testing. The 1.76 μm TiN-coated coupon had no post-coat finishing. The pins are machined from surgical grade Hostalen GUR-41 UHMWPe rod stock. The UHMWPe was not subject to a sterilization process. Dimensional specifications for the pins and coupons are given in Table 3. Each coupon is paired with three pins throughout testing.

A pin holder, secured on the floor of the containment cup (Figures 3, 4 and 5), holds three UHMWPe pins at 120° of separation making a planar surface for a coupon to rest upon. The coupon is suspended directly superior to the pins via a coupon holder. A motorized rounded-hex driver oscillates the coupon holder through 90° by interlocking with a hex-nut opening on the superior side of the coupon holder. The rounded-hex driver maintains a planar surface of contact in case of any minimal differences in height of the pins.

The containment cup is filled with distilled water to dissipate frictional heat and

TABLE 3: Materials

UHMWPe Pins

Material	Hostalen GUR-415 (surgical grade)	Diameter (mm)	6.35
		Cross sectional area (mm^2)	31.7
Molecular weight	3×10^6 minimum	Length (mm)	12.7
Density (g/cm^3)	0.933	Exposed length (mm)	3.2

Metal Coupons

Dimensions		Alloy	Coating	Pre-test Surface Finishing	Roughness (R_a, μm)
Diameter (mm)	31.75	Ti-6Al-4V ELI	TiN 1.76 μm	none	.08
Height (mm)	6.35		TiN 4.15 μm	DP-lapping	.11
			TiN 10.5 μm	DP-lapping	.07
		Co-Cr	none	DP-lapping	.03

to have a medium for the filtration and removal of wear debris from the system. Connected to the containment cup via ⅜ inch Masterflex tubing is a water pump and filtration system (Figures 3 and 5). Whatman #1 filter paper is used for the collection of wear debris. This is a medium-fast paper designed for medium crystalline retention. Distilled water is circulated through the system at 6 liters per hour and maintained at approximately 25°C (lab temperature) throughout the test cycle. The volume of the distilled water has minimal fluctuation throughout the test by continual replacement of evaporated water with fresh distilled water.

A testing load of 186 N is applied via an air cylinder to the bottom of the containment cup (Figures 3 and 5). This load is distributed onto 3 pins with cross sectional areas of 31.7 mm^2 each creating a contact stress of 1.95 GPa at the metal/UHMWPe interface. This is equivalent to the contact stress on a 32 mm femoral head under 2.5 times body weight of a 68 kg person, a common stress for the hip [5]. The tests are run up to 10 million cycles, each million cycles of testing being equivalent to 40 km sliding distance. The stroke of the system is 0.04 meters, an estimation of the stroke of the hip, at a rate of six cycles per second. This produces an average sliding speed of 0.24 meters per second. Six cycles per second has been shown to be a reasonable value for testing these materials, keeping the system well below pressure-

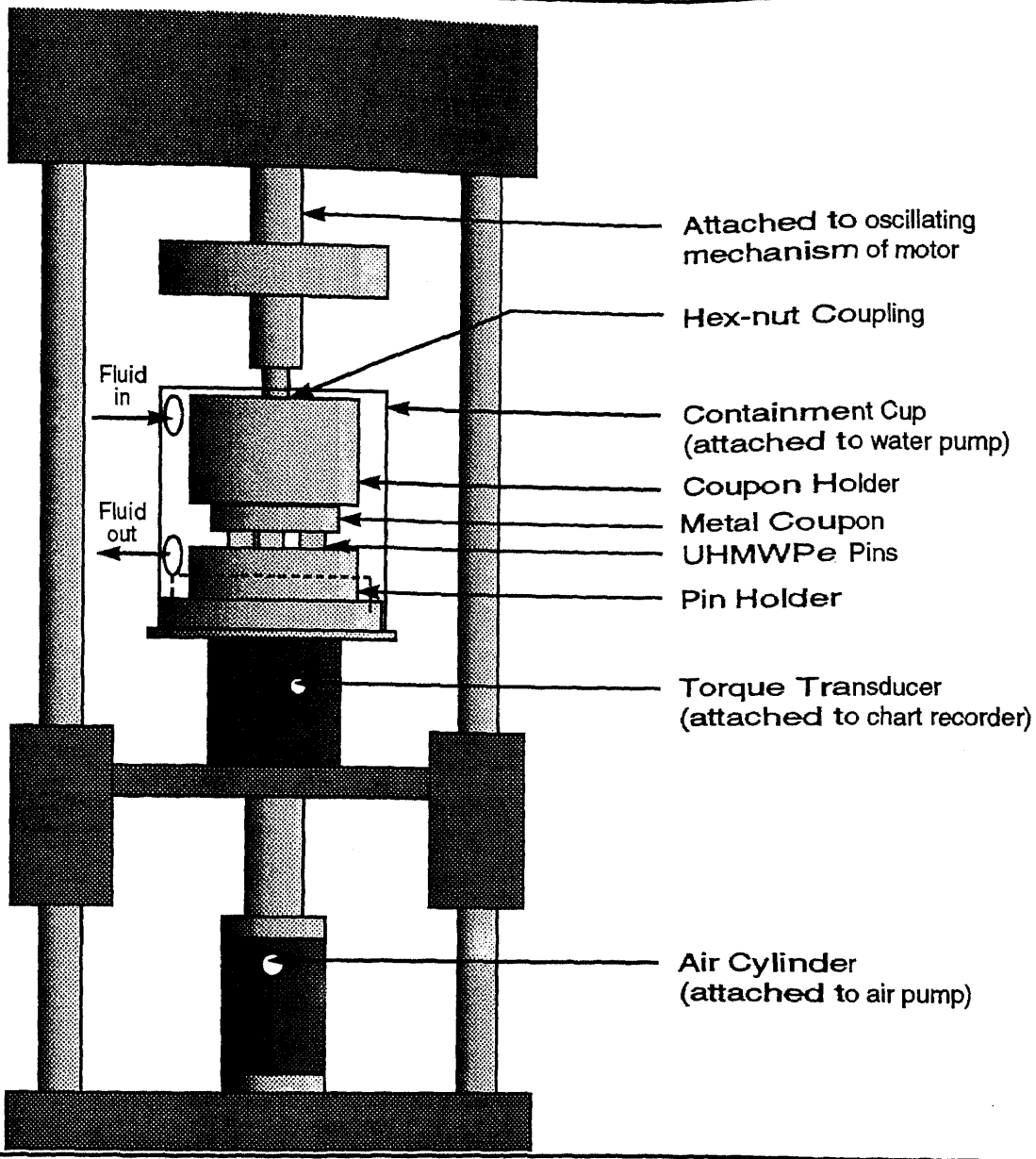

FIGURE 3: Oscillating Tribometer

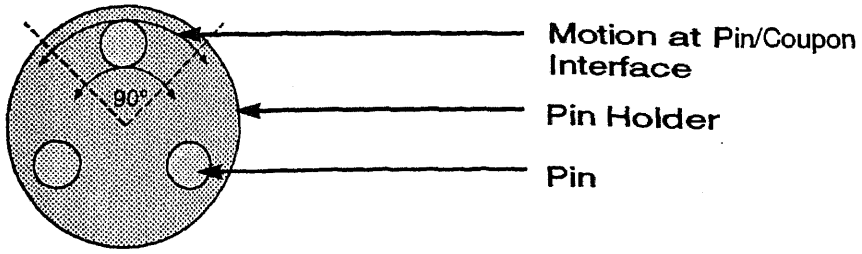

FIGURE 4: Cross Sectional View at Pin/Coupon Interface

(5a) Oscillation System

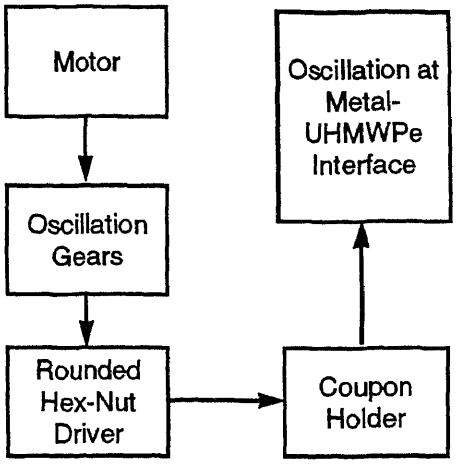

(5b) Loading System

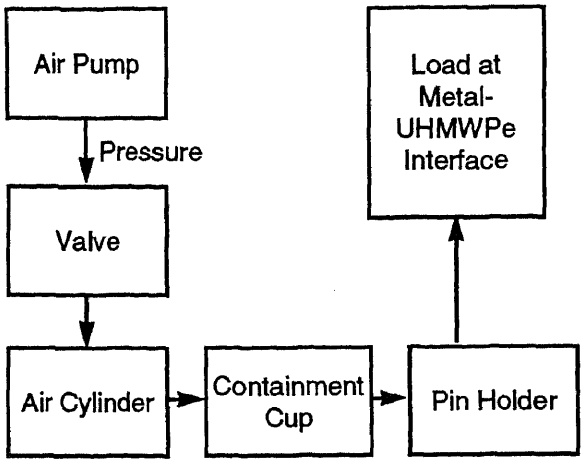

(5c) Cooling-Lubrication System

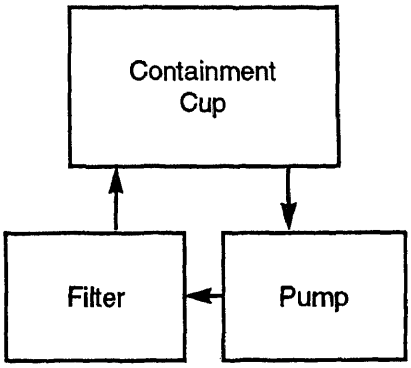

(5d) Monitoring System

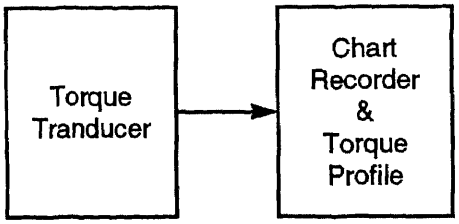

(5e) Tribometer Schematic

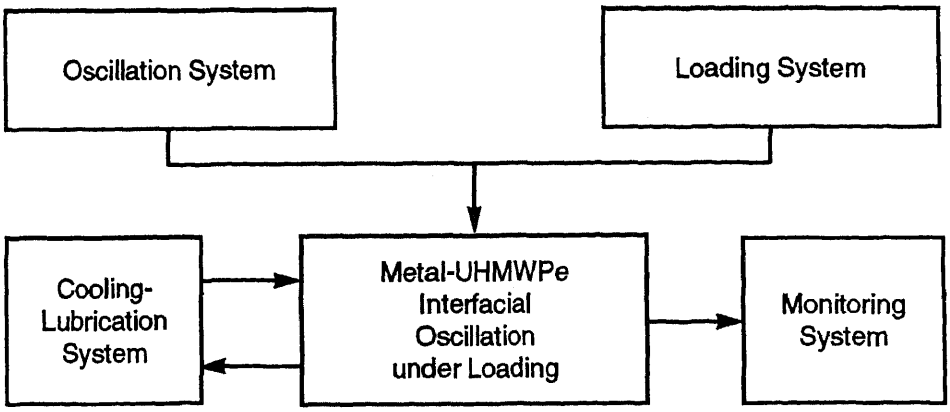

FIGURES 5a-e: Tribometer Schematics

velocity value limits [28]. Testing parameters are restated in Table 4.

TABLE 4: Test Conditions

Nominal contact stress/pin (GPa)	1.95	Frequency (cycles/sec)	6
Specific load/pin (N)	62	Number of cycles	Up to 10^7
Motion	Oscillatory	Environment:	
Oscillation angle (deg)	90	Solution	Flowing distilled water
Stroke (m/cycle)	0.04	Flow rate (l/h)	6
Sliding velocity (m/s)	0.24	Temperature (°C)	25

A Tranducer Techniques RTS-500 torque sensor, with a capacity of 1.92 N·m, is installed in the base of the tribometer, calibrated, and attached to the bottom of the containment cup (Figures 3 and 5). Connection to a Gould 2400S Chart Recorder provides a continuous record of the tangential force transmitted across the specimen interface.

Every 1 to 1.5 million cycles the testing is interrupted in order to make an evaluation of the materials' performances. Pin length is recorded and the pins are weighed on a Mettler H78 AR analytical balance with an accuracy of 100 μg. According to ASTM standards [29] each specimen is weighed three times to detect random errors in the weighing process. A visual observation and sketch are made of the coupon surface, noting any scratches, transfer film formation, and/or breach of the coating to the substrate surface.

After completing the study polarized light photomicroscopy is used to make a detailed record of surface conditions, concentrating on both worn and non-worn areas. Profilometries are also recorded across the worn and non-worn areas of the coupons with a Hommel Tester T1000C using a 1.5 mm and 4.8 mm scans. The three worn areas, or tracks (each corresponding to one pin), are each divided into two separate areas: mid-track and end-track. The mid- and end-tracks are distinguished to investigate variation in coating and substrate wear that may occur between sliding on the mid-track and the oscillation "turn around" region at the end-track. Figure 6 shows the division of the coupon into its different wear areas and also the placement of each of the pins, numbered 1 to 3.

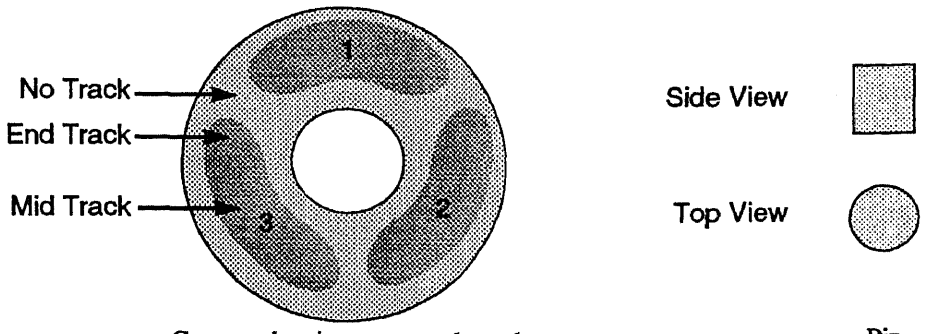

Coupon showing wear tracks and individual pin placement by number

FIGURE 6: Coupons and Pins

A soak control pin is submerged in distilled water during testing and removed and weighed with the test pins to determine fluid absorption (S) in grams. Since fluid absorption masks the actual mass loss due to wear, S is subtracted from the interval's recorded mass (M_R) of the test pins, converting an apparent mass gain or loss into an actual mass loss, and giving the actual mass (M_A) of the pin.

$$M_A = M_R - S \quad (1)$$

The mass loss (M_L) on a pin is described as the M_A at a specific interval subtracted form the beginning mass of the pin (M_B).

$$M_L = M_B - M_A \quad (2)$$

While UHMWPe wear results in a change in the pin height, it is distinct from height changes due to plastic deformation (i.e. creep) in that it results in the removal of material in the form of polymeric debris particles, causing a loss in mass from the specimen. Therefore, records of the change in pin length during the test are not utilized in determining wear in the tribo system. As a result, volumetric wear (V) is used and calculated with the density (ρ) of the UHMWPe and the actual mass loss on the pins (M_L):

$$V = M_L/\rho = M/0.933 = 1.072 \times M_L. \quad (3)$$

The wear rate (R) is described as the volumetric wear (V) per interval (n) of sliding distance (X), as measured in kilometers:

$$R = \frac{V_n - V_{n-1}}{X_n - X_{n-1}} \tag{4}$$

Torque is established from the paper output of the chart recorder which graphically displays changes in torque. The number of units of displacement across a central line of the output are multiplied by a calibration value of 0.0576 N·m to give the torque. Six cycles within a one second period are averaged together to calculate the experimental torque. This torque (τ) was converted to a coefficient of friction (μ) by the equations:

$$\mu = \text{Frictional force/Normal force} \tag{5}$$

$$\mu = \tau \cdot \text{Moment Arm}^{-1} \cdot \text{Normal force}^{-1} \tag{6}$$

$$\mu = 0.423\ (N^{-1} \cdot m^{-1}) \times \tau\ (N \cdot m). \tag{7}$$

CHAPTER 4
RESULTS

Figure 7 shows the performance of all TiN-UHMWPe systems and the Co–Cr-UHMWPe system in wear control. At 10 million cycles the 1.76 μm TiN-UHMWPe has a volumetric loss of 1.71 mm^3, the 4.15 μm TiN-UHMWPe loses 3.43 mm^3, and the 10.5 μm TiN-UHMWPe has 3.22 mm^3 loss. Co–Cr-UHMWPe has a volumetric loss of 5.36 mm^3. The 1.76 μm TiN-UHMWPe has 32 percent the wear of CoCr, while the 4.15 μm TiN-UHMWPe and 10.5 μm TiN-UHMWPe have 64 percent and 60 percent the wear, respectively.

The performance of each pin against its respective counterface is given in Figure 8. All the pins coupled with the 1.76 μm and 10.5 μm TiN-coated coupon are consistent with one another in volumetric wear. The pins with the 4.15 μm TiN-coated coupon and the Co–Cr coupon show more drift. In this latter case, the pin in placement 2 (see Figure 6) does not follow the trends of pins in placement 1 and 3, and at test conclusion has almost double the wear those pins in their respective tests. At test end the volumetric wear ratios for the pins in these tests are as follows: for the 4.15 μm TiN-UHMWPe system: pin 2/pin 1 = 1.77, pin 2/pin 3 = 2.29; and for the Co–Cr-UHMWPe system: pin 2/pin 1 = 2.20, pin 2/pin 3 = 2.20).

The overall wear rates for the four experimental systems is given in Figure 9. Initially, the Co–Cr-UHMWPe has the highest rate, approximately 28 $mm^3/km \times 10^{-3}$. The 4.15 μm TiN-UHMWPe has the next highest with a little under 14 $mm^3/km \times 10^{-3}$, less than half that of the Co–Cr, while the 1.76 μm TiN-UHMWPe and 10.5 μm TiN-UHMWPe experience very little wear (approximately 2 $mm^3/km \times 10^{-3}$ each), only 7 percent of that of Co–Cr-UHMWPe.

After some light wear (under 8 $mm^3/km \times 10^{-3}$) from all TiN-UHMWPe and the Co–Cr-UHMWPe systems another stage of wear begins. This stage, which starts at

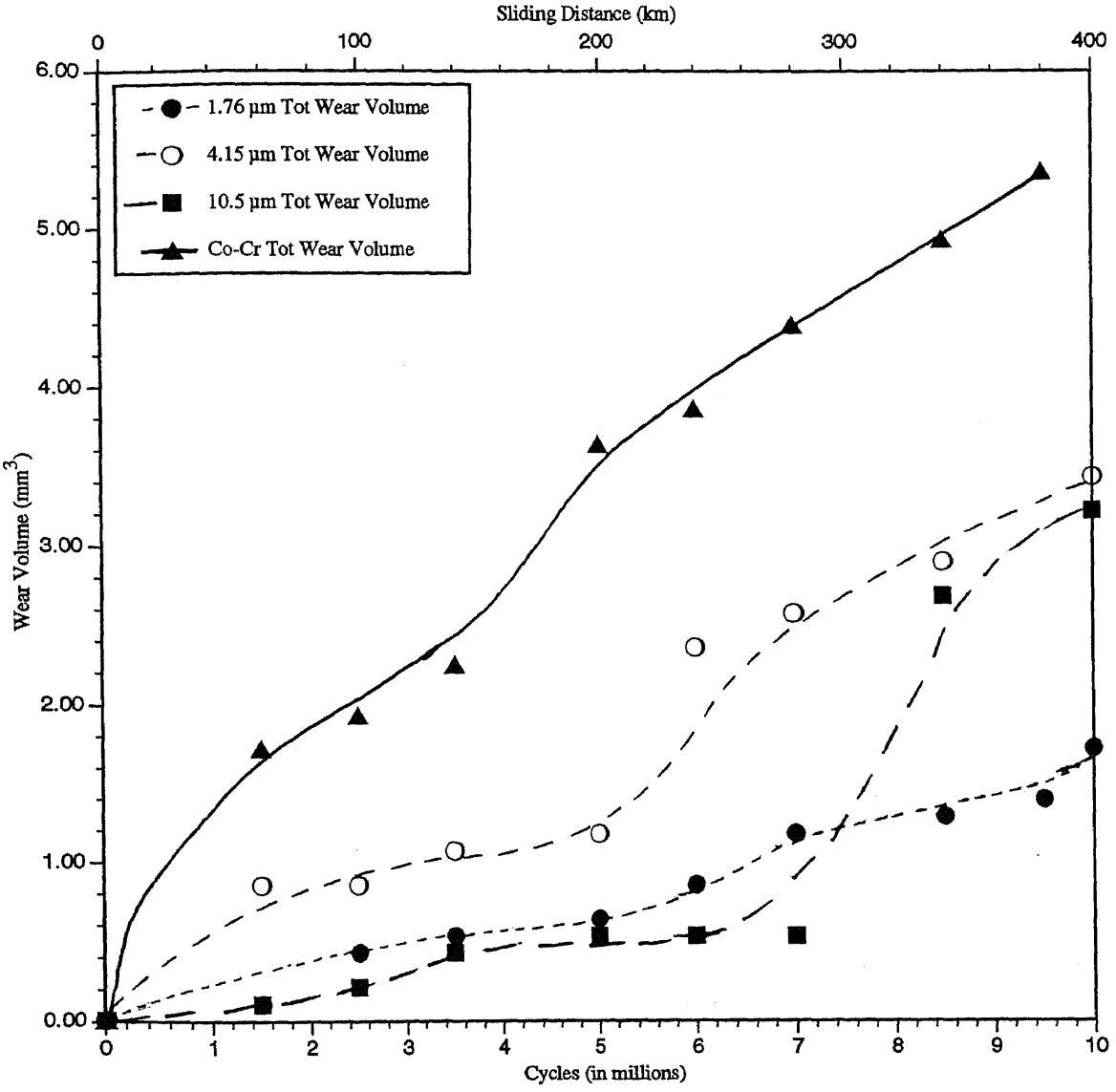

FIGURE 7: Volumetric Wear of UHMWPe Against Test Coupons (Combined Results of All Pins)

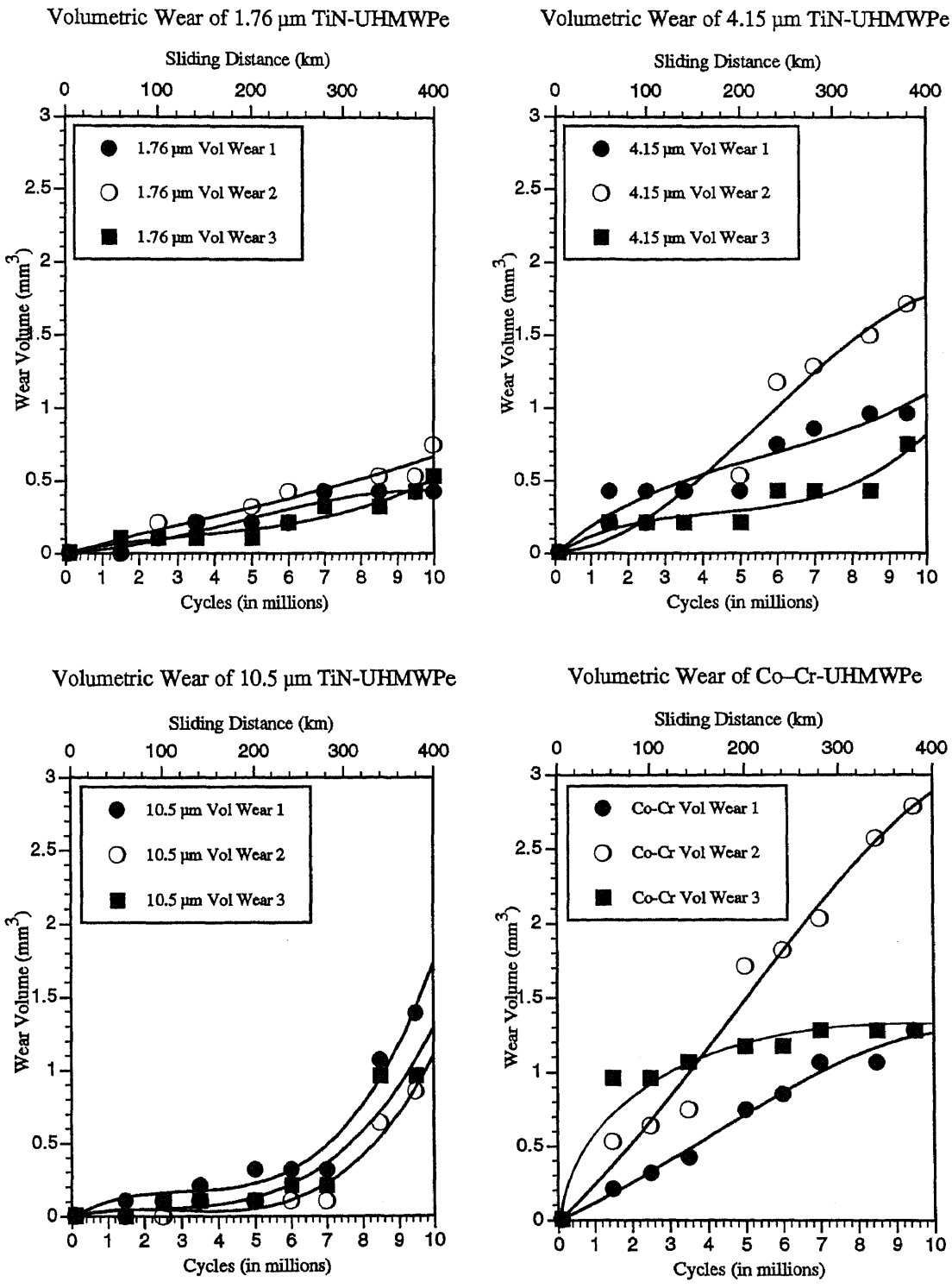

FIGURE 8: Volumetric Wear of Individual UHMWPe Pins Against Test Coupons.

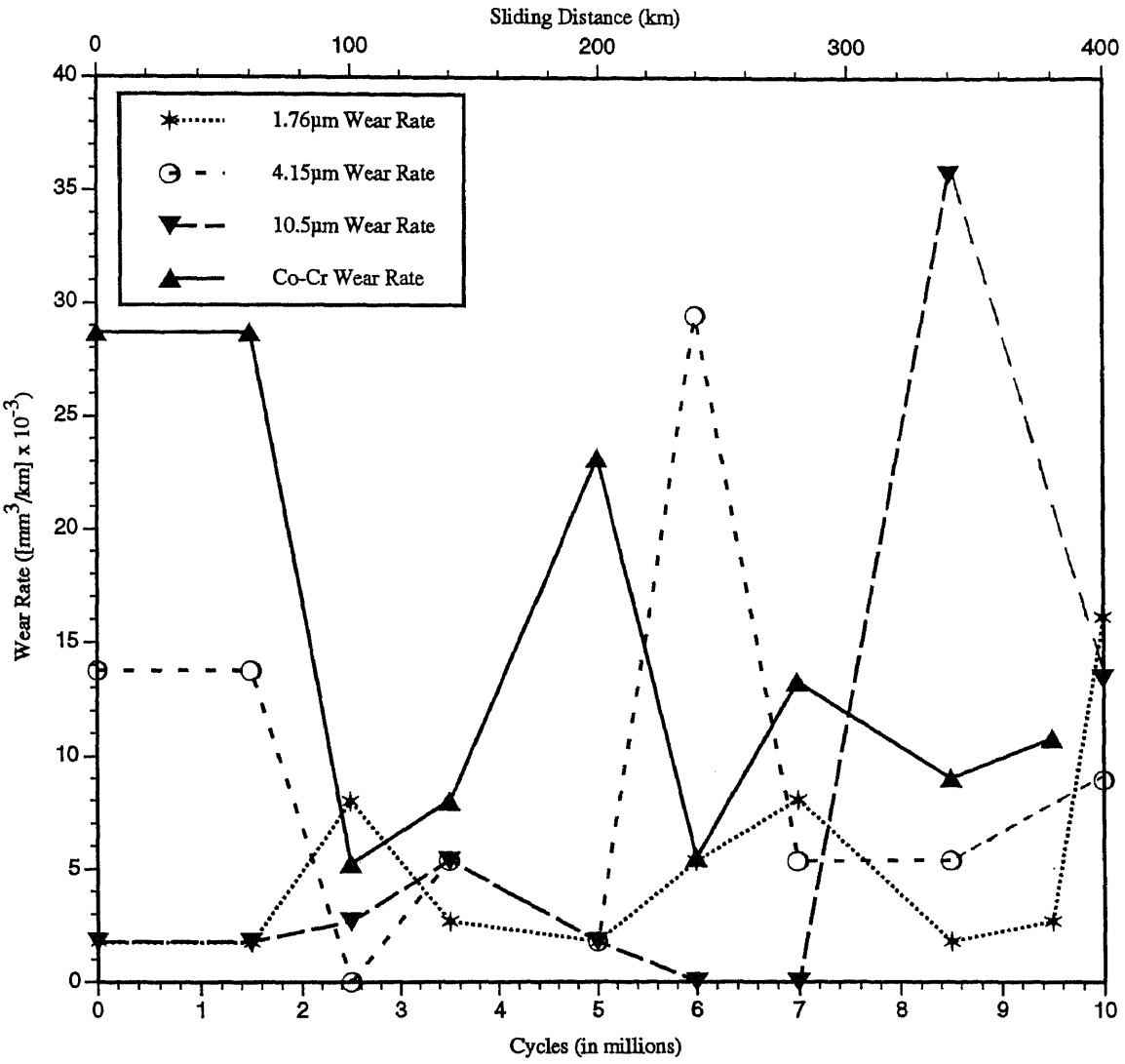

FIGURE 9: Total Wear Rate of UHMWPe on Test Coupons (Sum of Individual Pin Wear Rates to Derive a Total Rate for Each Coupon)

various sliding distances depending on the coupon being tested, is marked by highly accelerated wear of the UHMWPe. It occurs first for Co–Cr-UHMWPe and starts about 3.5 million cycles (or 140 km of sliding distance). The rate falls to approximately 5 $mm^3/km \times 10^{-3}$ after the high initial rate and then again rises to 23 $mm^3/km \times 10^{-3}$. The 4.15 μm TiN-UHMWPe couple is the second to undergo an acceleration in wear. At 5 million cycles (or 200 km of sliding distance) the wear rate rises from 2 $mm^3/km \times 10^{-3}$ to 30 $mm^3/km \times 10^{-3}$. The 10.5 μm TiN-UHMWPe has accelerated wear after a period little or immeasurable wear for 7 million cycles (or 280 km of sliding distance). The rate becomes 35 $mm^3/km \times 10^{-3}$. The 1.76 μm TiN-UHMWPe does not undergo as distinct a period of accelerated wear throughout the 10 million cycles of testing, but there is evidence one begins toward the end of the test: the rate goes from 3 $mm^3/km \times 10^{-3}$ at 9.5 million cycles to 16 $mm^3/km \times 10^{-3}$ at 10 million cycles.

In the three cases which undergo a clear stage of very high wear, the rates fall sharply afterward. The Co–Cr-UHMWPe rate ended lower than it was previous to accelerating, declining to 76 percent from the peak rate. The 4.15 μm TiN-UHMWPe and 10.5 μm TiN-UHMWPe also have steep drops in wear rates, decreasing 82 percent and 62 percent from peak rates, respectively. The 1.76 μm TiN-UHMWPe does not experience a decrease in wear at test end. The wear rates for each pin are shown in Figure 10. Portions of Figures 9 and 10 distinguished by a wear rate of zero do not indicate no wear but rather wear not measurable within the accuracy of the balance, a source of experimental error.

The coefficients of friction for various instances over the 10 million cycles of testing are given in Figure 11. For 1.76 μm TiN-UHMWPe the range is 0.055–0.106 (average value = 0.073), for the 4.15 μm TiN-UHMWPe the range is 0.050–0.085 (average value = 0.068), for the 10.5 μm TiN-UHMWPe the range is 0.049–0.080 (average value = 0.067), and for the Co–Cr-UHMWPe the range is 0.054–0.080 (average value = 0.063). The recorded coefficients of friction are momentary, and not continuous

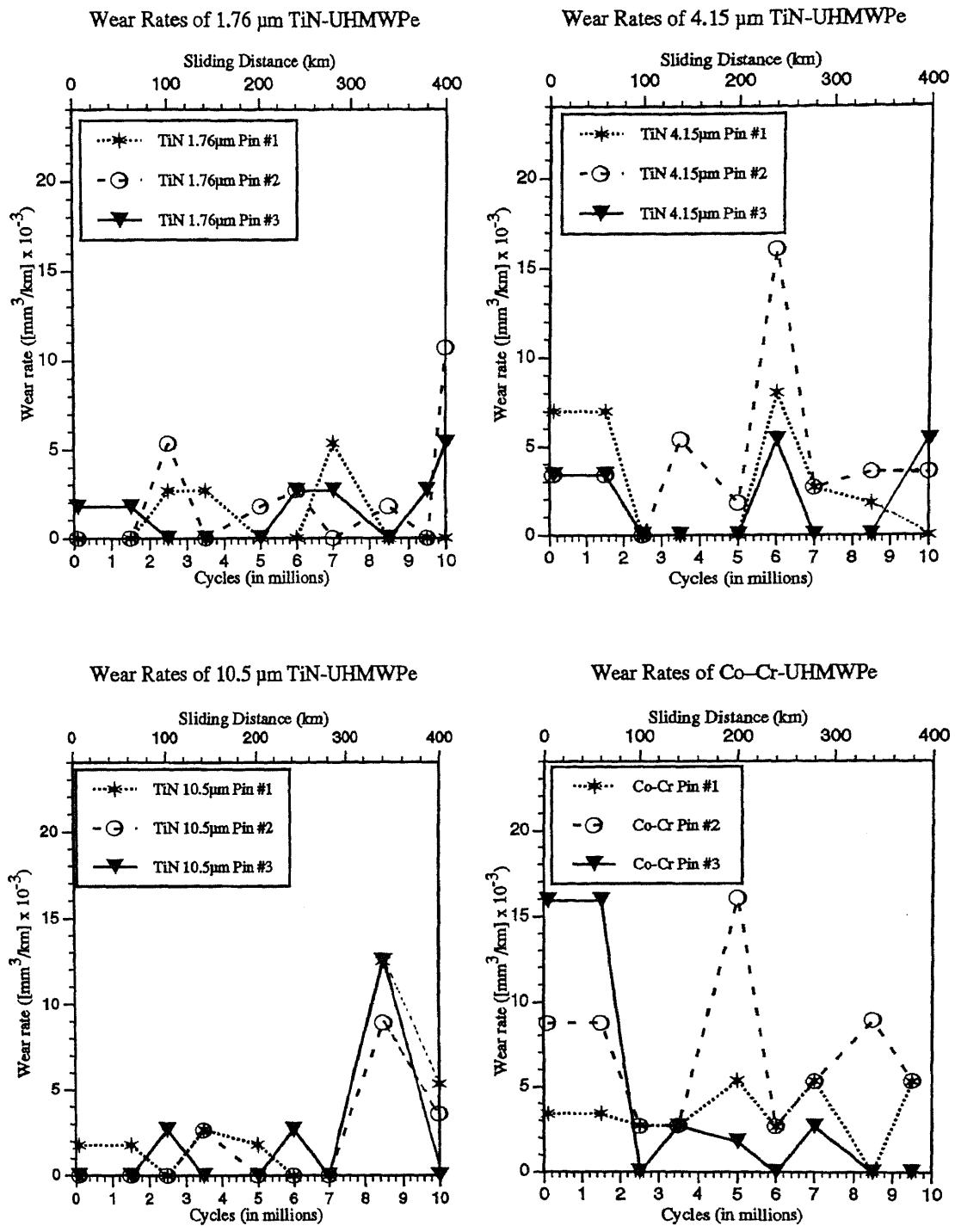

FIGURE 10: Wear Rate of Individual UHMWPe Pins on Test Coupons

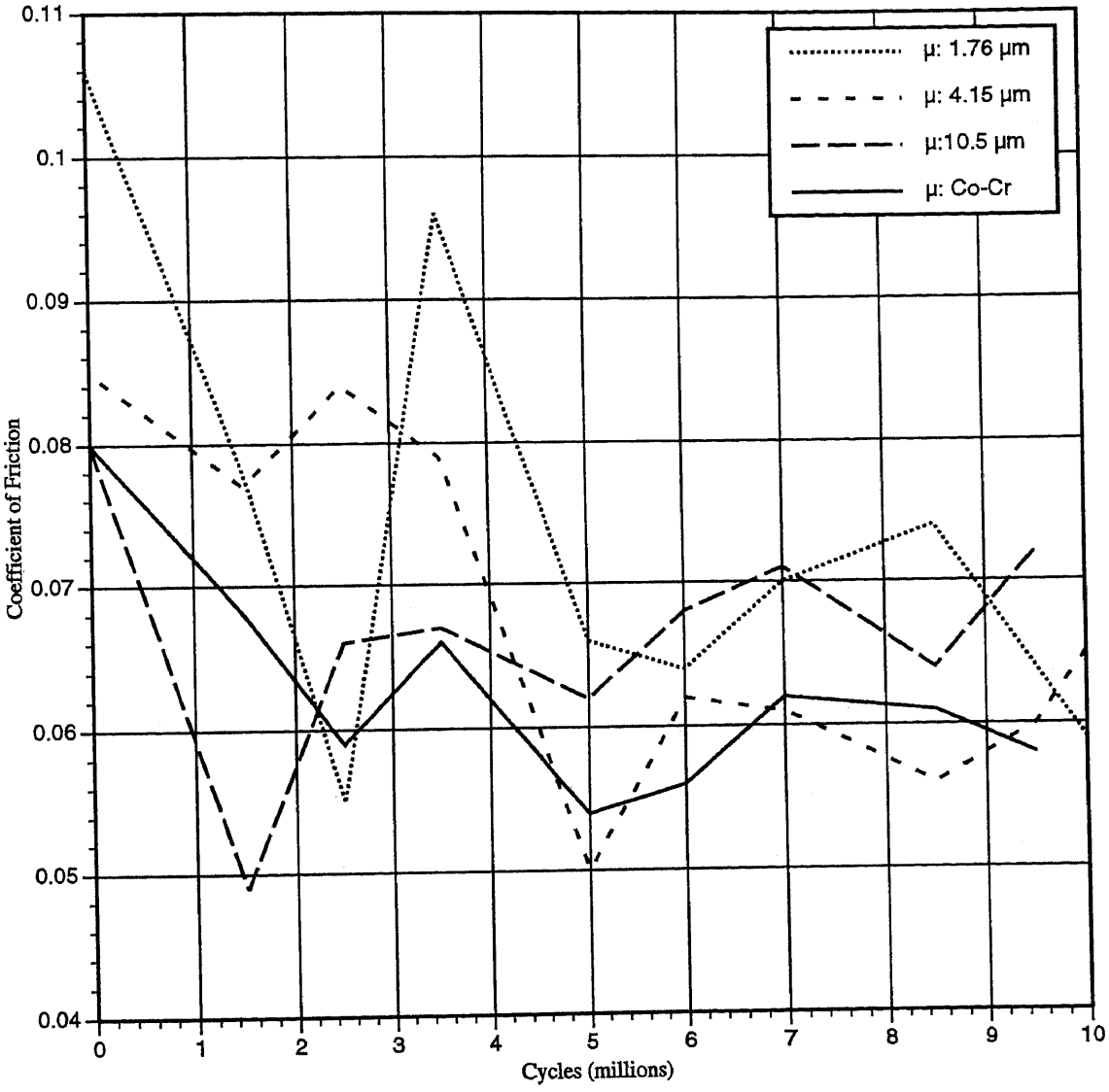

FIGURE 11: Coefficient of Friction Over 10 Million Cycles of Testing

as the graph may indicate. Other changes in the coefficient may have occurred between readings.

Figure 12 shows the performance of each coupon in its resistance to wear on track 3. At test conclusion none of the TiN–coated coupons has scratches greater than 2 μm in depth, while the Co–Cr coupon's scratches are all greater than 2 μm—with some even deeper than 10 μm. With thicker TiN coatings the number of scratches increases. There is no significant difference between the mid- and end-track performance on any of the coupons.

Table 5 presents the profilometry data (measured in μm) from the Hommel Tester T1000C. The R_a value is the arithmetic mean roughness. This is determined from deviations about a 'center' line within the scan length of 1.5 mm. The R_m value is the maximum individual peak-to-valley dimension and the R_z value is the average height difference between the five highest peaks and five lowest valleys contained within the scan length. The information given in this table represents a single scan across each of the three separate areas of interest shown in Figure 6. For the mid- and end-track this scan was completely within the bounds of the outline of the wear track. The data comes from a separate pass than that used for Figure 12 (a 4.8 mm scan), so numerical values differ; nevertheless, the trends are the same. The TiN-coated coupons held up very well over the testing period, maintaining pre-test surface quality in the 1.76 μm and 4.15 μm TiN coatings. The 10.5 μm TiN coating shows slight deterioration while the Co–Cr evidences marked deterioration.

TABLE 5: Coupon Profilometry at Test End

	CoCr			1.76 μm TiN			4.15 μm TiN			10.5 μm TiN		
	R_a	R_m	R_z	R_a	R_m	R_z	R_a	R_m	R_z	R_a	R_m	R_z
No track	0.03	0.24	0.18	0.08	1.06	0.69	0.11	1.64	0.92	0.07	1.18	0.64
Mid wear track	0.59	7.44	4.58	0.07	0.78	0.60	0.08	1.54	1.76	0.14	1.64	1.20
End wear track	0.70	7.56	4.27	0.09	0.90	0.68	0.06	0.74	0.49	0.19	1.62	1.38

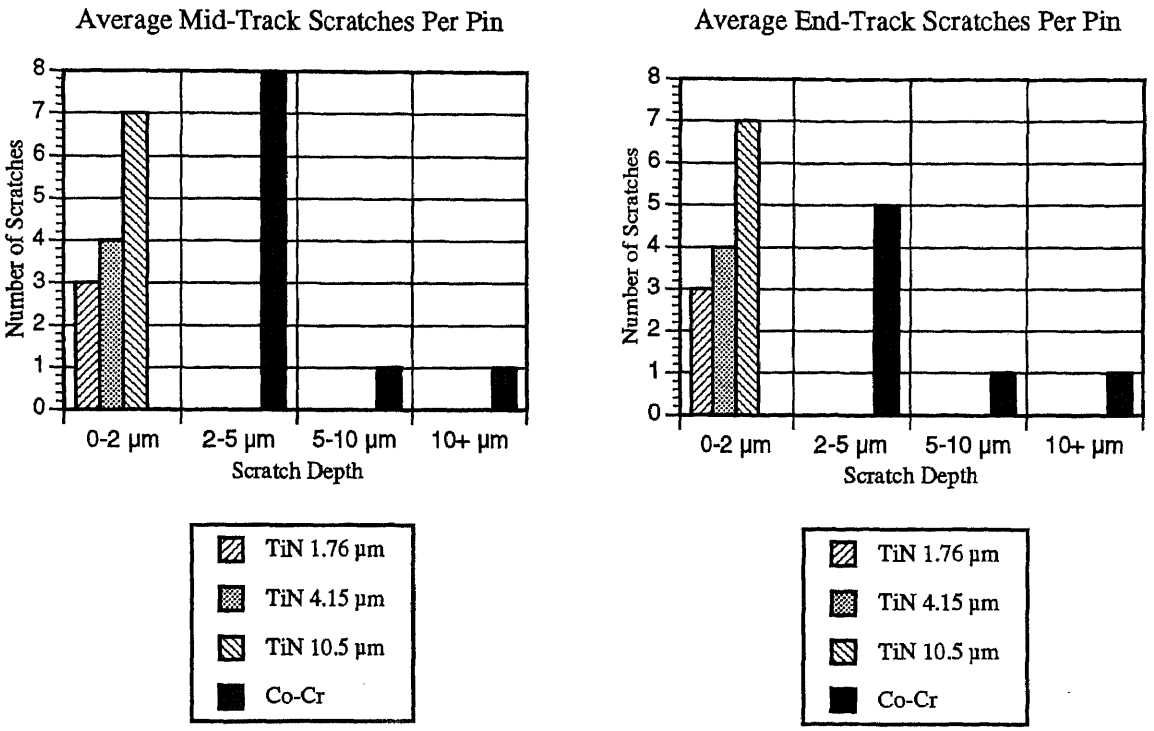

FIGURE 12: Profilometry Data From Scan Across Track 3 on All Coupons

Photographic evidence (Figures 13-16) exhibits the pre- and post-test conditions of all coupon surfaces. Adhesion of the coating is maintained on all TiN coupons. There is no evidence of surface fracture or crazing. A slight burnishing of the wear track on the TiN surface indicates minor abrasive wear by TiN wear debris particles. This is most evident on the 10.5 μm TiN coating. Polyethylene adheres in patches, increasing in frequency and size with an increase in coating thickness. UHMWPe induced scratches are minor on the 1.76 μm and 4.15 μm TiN coatings, but the 10.5 μm coating has a few scratches which evidence minor surface deterioration. The Co–Cr coupon shows a marked surface deterioration, with many deep and wide scratches and an almost continuous UHMWPe film.

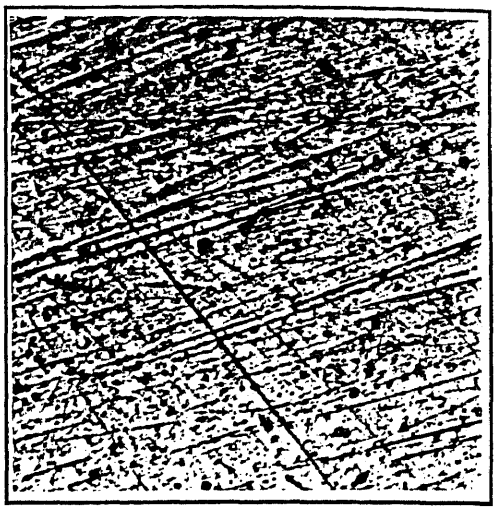

FIGURE 13a: TiN 1.76 μm Coating Pre-test Condition Under 240x Magnification. Notice multi-directional scratches which are remnants of surface finishing prior to coating .

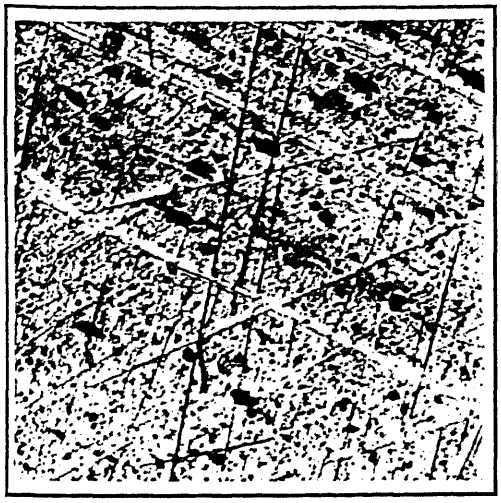

FIGURE 13b: TiN 1.76 μm Coating at 10 Million Cycles Under 240x Magnification. Small UHMWPe patches, slight discoloration due from burnishing due to abrasion by TiN wear particles, and light scratches in the sliding direction caused by UHMWPe are evident.

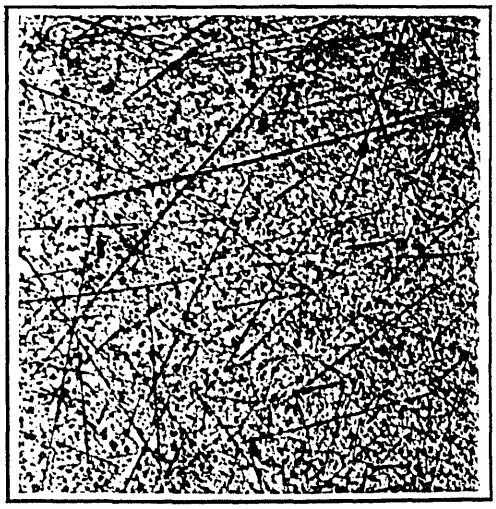

FIGURE 14a: TiN 4.15 μm Coating Pre-test Condition Under 240x Magnification. Sub-coating scratches are present, but less evident due to filling by TiN ceramic.

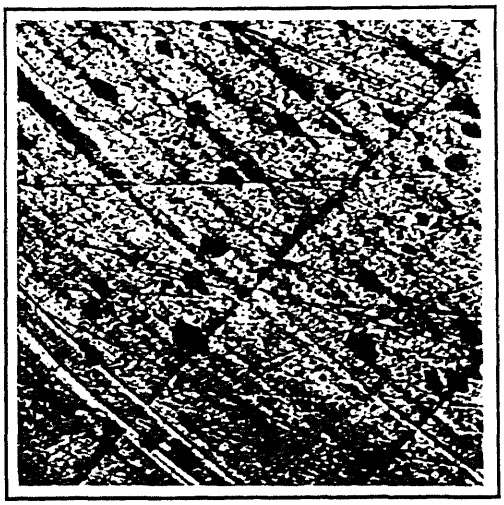

FIGURE 14b: TiN 4.15 μm Coating at 10 Million Cycles Under 240x Magnification. Patches of UHMWPe are distributed more heavily than on the TiN 1.76 μm coating in FIGURE 13b.

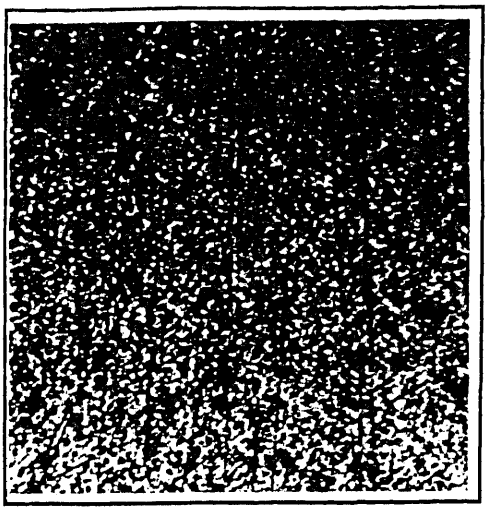

FIGURE 15a: TiN 10.5 μm Coating Pre-test Condition Under 240x Magnification. Pre-coating scratches are not easily distinguished because they have been filled by TiN coating.

FIGURE 15b: TiN 10.5 μm Coating at 10 Million Cycles Under 240x Magnification. An increasing amount of UHMWPe is present on the surface. Burnishing, due to TiN wear debris particles, has given the entire surface as bronzed look. This coupon had the deepest scratches of the TiN coated coupons, one of which is evident here.

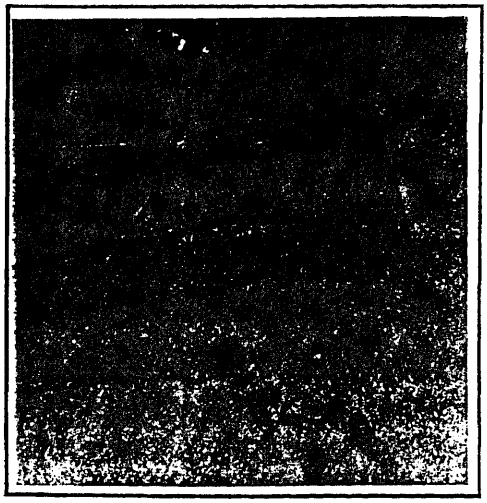

FIGURE 16a: Co-Cr Pre-test Surface Condition Under 240x Magnification. The absence of major scratches evidences the differences between the Co-Cr surface and the TiN coated surfaces as recorded during pre-test profilometries.

FIGURE 16b: Co-Cr Surface at 9.5 Million Cycles Under 240x Magnification. Scratches are deep and wide and the UHMWPe film covers the entirety of the surface.

CHAPTER 5
DISCUSSION

Experimental error in a test such as this can be high due to the limits of scale accuracy. The Mettler balance utilized is accurate to 100 μg, a not unusual measurement of mass loss on a pin during low wear intervals of testing. In calculating mass loss four separate weighings must be performed (soak control pin initial mass, soak control pin interval mass, test pin initial mass, test pin interval mass) on each pin, each weighing having the possibility of ±100 μg error. Furthermore, overall volumetric wear and overall wear rates are calculated using the combined values of three test pins, compounding the margin for error. However, each pin was weighed three times to reduce such error and the large number of mass readings over the testing insures, in part, validity in the results. Error associated with water absorption is not a factor to affect sufficiently the calculation of wear loss. If the pins over the test lost a substantial percentage of their mass due to wear, water absorption of the soak control pin would not be representative of the test pins. This is not the case. As the pins at test conclusion lose less than 0.5 percent of their mass due to wear, the water weight gain from the soak control is representative of the water weight gain of the test pins throughout the test due to their proximity in size. Mass gain due to water absorption was minimal over the entire test, on the order of 100–200 μg and only 0.027–0.054 percent the total pin mass.

Only at the initial portion of the testing, when mass loss was very small (on the order of 100 μg) is a significant error possible. However at higher wear rates and later in the testing when cumulative mass loss is greater, the experimental error diminishes becoming less important. Throughout the test experimental error is not sufficient to inhibit evaluation of the materials.

The first stage of testing (up to 2 million cycles) is a transient stage in which 'bedding-in' occurs for the counterfaces, smoothing out any major roughnesses on the

pins left over from the machining process. Therefore, the high initial rates are expected. The subsequent sudden and temporary acceleration of the wear rate, however, is a strange phenomenon. This reaction may be an artifact of pin-on-disk wear testing as similar results have been reported with such testing. McKellop [31] using Co–Cr coupons and UHMWPe noticed accelerated wear for a period of 200,000 cycles "with the coefficient of friction as high as 0.24 and a heavy transfer layer covering about 50 percent of the contact area. Eventually the [polyethylene] transfer material was rubbed away and the friction returned to its normal level." Rostoker and Galante [32] recorded a similar occurrence with stainless steel on graphite-filled polyethylene. Running a test up to 5 million cycles, they state "at a late stage there is an unexpected and unexplained change due to a relatively high wear rate which is at least an order of magnitude higher."

An explanation may be that over the longer testing periods a transfer film of UHMWPe begins to reside upon the metal coupon. This build-up begins a period of adhesive wear which quickly wears at the pins. A steady transfer film is built up over a few million cycles until the shear stress at the areas of adhesion becomes large enough to remove the transfer film and return the wear rate to 'normal' levels. The data that has been gathered could be explained by such events. While transfer films are observed *in vivo*, whether or not such dramatic variations in wear are present in physiological conditions has not been determined.

The reduction in wear seen with the TiN-UHMWPe system has been previously linked to a low coefficient of friction. Pappas [28] suggested that the reduced wear of TiN-UHMWPe over Co–Cr-UHMWPe is in part a result of a lower coefficient of friction achieved using a TiN coating. He noted that a "substantial increase in smoothness" is obtainable with thin TiN films on a highly polished Ti–6AL–4V substrate. The current study, however, does not find a relationship between the coefficient of friction and the wear results. The wear is indeed reduced with TiN *but* a reduction in friction does not occur. Martinella [27] concurs with such findings. He has found the coefficient of

friction to fluctuate considerably during oscillating pin on disk testing—in the range of 0.02–0.2. "No quantitative relationship was found between the frictional coefficient and the wear rate of UHMWPe." McKellop [31], is also in agreement employing the usual test configurations as well as simulators. Furthermore, Bull [23], also using Ti–6AL–4V coupons, found that the friction measured in [his] test was about the same for TiN-coated and uncoated disks, but the wear was much greater for the uncoated disk. Reduced wear cannot, therefore, be attributed in large part to a reduced coefficient of friction. However, the coefficient of friction cannot be discounted as unimportant. It must be realized that the coefficient of friction is both material and condition specific. The pre-test surface quality of the TiN-coated coupons (R_a between .07 and .11), which did not approach that of the Co–Cr (R_a =.03), may have been an inhibiting factor on friction reduction.

Additionally regarding smoothness, the lowest total wear volume caused by a TiN coating was that of 1.76 μm coating. It is not difficult to reconcile the 1.76 μm coating having the highest average and peak coefficient of friction and also inducing the least wear. By the nature of the 'thinness' of this coating it may have actually become smoother during the testing leading to better results. Initial abrasive wear could remove the microdroplets which had been a factor in surface roughness. The high coefficient of friction which is recorded early in the test and falls dramatically by mid test and remains low. Furthermore, on all TiN-coated coupons measured pre-test roughness is not correlative to wear, whereas thinness of coating seems to be inhibitory to scratch formation which is evidenced by the photomicroscopy.

There are other unexplained results of this study. Pin 2 exhibited anomalous wear behavior in two of the tests. It is difficult to explain this behavior except to look toward a misalignment between the coupon holder and pin holder which was not corrected by the use of the rounded-hex driver. Nevertheless, if loading was higher on pin 2 the total wear characteristics of the system (i.e. the combined volumetric wear of pins 1, 2, and 3)

should remain at the same level, and the overall results should remain unchanged.

Long scratches in the sliding direction which outline the wear tracks appear to be artifacts of tests that use repetitive tracking. The presence of such scratches are confirmed by others doing similar testing [27, 28, 30] and are not found on retrieved implants [28]. The profilometries give insight into the scratches at the center of the wear track. The TiN coating maintains its integrity and it is this factor which is responsible for keeping the abrasive wear low on the TiN-UHMWPe systems.

CHAPTER 6
CONCLUSIONS AND SUGGESTIONS

TiN-coated coupons with pre-test surfaces rougher than their Co–Cr counterpart have up to a two-thirds reduction in UHMWPe wear over Co–Cr. This seems partly to be a result of the TiN coatings' resistance to transfer film formation, a 'polymer-phobia,' and a property which is more effective at thinner coating thicknesses. Further, greater reductions in wear have been found with thinner coatings, which may be a result of thinner coatings equating with smoother coatings, or the ability of thinner coatings to become smoother over time. Smoother TiN-coated surfaces (at the level of implant quality, $R_a \leq 0.05$) are possible and a projection can be made that this will enable further wear reduction. But it does not appear that TiN's smoothness is solely responsible for the improved wear profile seen with TiN/Ti-6Al-4V on UHMWPe. Rather TiN's hardness, scratch resistance, and 'polymer-phobic' properties combine to foster a superior tribo-surface for interaction with UHMWPe.

Future research should address the issue of counterface smoothness, testing uniformly smooth TiN/Ti-6Al-4V coating/substrate systems and Co–Cr. Only then will the actual improvement in wear reduction be quantitatively realized.

Substantial improvements in wear control can be obtained using a TiN/Ti-6Al-4V coating substrate system. Exactly how this is fostered is still not clear and a definitive answer would be helpful for further improvements in wear reduction.

BIBLIOGRAPHY

[1] Williams, D.F. & Roaf, R., *Implants in Surgery*, W.B. Saunders Co. Ltd., London (1973).

[2] Lynch, W., *Implants: Reconstructing the Human Body*, Van Nostrand Reinhold Company, New York (1982).

[3] Brettle, J., *A Survey of the Literature on Metallic Surgical Implants*, United Kingdom Atomic Energy Authority, AWRE Metallurgy Division, DHS Project A129 (1969).

[4] Charnley, J., Factors in the design of an artificial hip joint, *Symposium on Lubrication and Wear in Living and Artificial Human Joints*, Institute of Mechanical Engineers, London (1967).

[5] Friedebold, G. & Kölbel, R., State of the art of hip and knee joint replacement, *Engineering in Medicine 2: Advances in Artificial Hip and Knee Joint Technology*, Edited by M. Schaldbach and D. Hohmann, Springer-Verlag, Berlin (1976).

[6] Charnley, J. et al, Analysis of the vertical component of force in normal and pathological gait, *Journal of Biomechanics*, 5, 11 (1972).

[7] Black, J., *Biological Performance of Materials: Fundamentals of Biocompatibility*, Ch.11, Marcel Dekkar, New York (1981).

[8] Isaac, G. H. et al, A tribological study of retrieved hip prostheses, *Clinical Orthopaedic and Related Research*, 276, p.116-125 (1992).

[9] Wroblewski, B. M., Wear and loosening of the socket in the Charnley low-friction arthroplasty, *Orthopedic Clinics of North America*, 19(3), p.627-630 (1988).

[10] Rimnac, C. M. et al, Acetabular cup wear in total hip arthroplasty, *Orthopedic Clinics of North America*, 19(3), p.631-636 (1988).

[11] Wright, T. M. et al, Wear of polyethylene in total joint replacement: observations from retrieved PCA knee implants, *Clinical Orthopaedic and Related Research*, 276, p.126 (1992).

[12] Collier, J.P. et al, The biomechanical problems of polyethylene as a bearing surface, *Clinical Orthopaedic and Related Research*, 261, p.107 (1990).

[13] McCoy, T. M. et al, A fifteen year follow-up study of one hundred Charnley low friction arthroplasties, *Orthopedic Clinics of North America*, 19(3), p.467-476 (1988).

[14] Suire et al, Method for manufacturing surgical implants at least partially coated with a layer of metal compound, and implants manufactured according to said method, United States Patent #4,790,851 (1988).

[15] Hayashi, K. et al, Evaluation of metal implants coated with several types of ceramics as biomaterials, *Journal of the Society of Biomaterials*, 23, 11 (1989).

[16] Multi-Arc Scientific Coatings, TiN Coatings for Surgical Implants, Rockaway, NJ

[17] Paquette, W., Coating technology for progressive stamping, reprinted from Stamping Quarterly (Summer 1989).

[18] Holleck, H., Material selection for hard coatings, *Journal of Vacuum Science Technology A*, 4 (6), p. 2661-2669, (1986).

[19] Coll, B. & Jacquot, P., Surface modification of medical implants and surgical devices using TiN layers, Surface and Coatings Technology, 36, p. 867-878, (1988).

[20] Mack, M., Surface Technology: Wear Protection, Interatom, (1990).

[21] Endotec, UltraCoat™ brochure, Issue date February, 1990.

[22] Vingsbo, O., Fundamentals of friction and wear, *Engineered Materials for Advanced Friction and Wear Applications Conference Proceedings*, ASM International, (1988).

[23] Bull, S. J., & Rickerby, D. S., The sliding wear of titanium nitride coatings, Surface and Coatings Technology, 41, p.269-283, (1990).

[24] Bull, S. J., & Rickerby, D. S., New developments in the modelling of the hardness and scratch adhesion of thin films, Surface and Coatings Technology, 42, p.149-164, (1990).

[25] McKellop, H. et al, Friction and wear properties of polymer, metal and ceramic prosthetic joint materials evaluated on a multi-channel screening device, *Journal of Biomedical Materials Research*, 15, p.619-653 (1981).

[26] Martinella, R. & Giovanardi, S., Chevallard, G., & Villani, M., Wear behaviour of nitrogen-implanted and nitrided Ti-6Al-4V alloy, Materials Science and Engineering, 69, p. 247-252, (1985).

[27] Martinella, R. & Giovanardi, S., Wear of ultrahigh molecular weight polyethylene sliding against surface-treated Ti6Al4V, AISI 316 Stainless Steal and Vitallium, Wear, 133, p. 267-279, (1989).

[28] Pappas, M. J. et al, Comparison of wear of UHMWPe cups articulating with Co-Cr and Ti-Ni coated, titanium femoral heads, *Transactions of the Society of Biomaterials*, Vol. 3 (May 1990).

[29] *ASTM Standard Practice for Reciprocating Pin-on-flat Evaluation of Friction and Wear Properties of Polymeric Materials for Use In Total Joint Prosthesis*, Designation: F732-82.

[30] McKellop, H. A. & Röstlund, T.V., The wear behavior of ion-implanted Ti-6Al-4V against UHMW polyethylene, Journal of Biomedical Materials Research, 24, p.1413-1425 (1990).

[31] McKellop, H. et al, Wear characteristics of UHMW polyethylene: A method for accurately measuring extremely low wear rates, *Journal of Biomedical Materials Research*, 12, 895-927 (1978).

[32] Rostoker, W. & Galante, J.O., Some new studies of the wear behaviour of ultra high molecular weight polyethylene, *Journal of Biomedical Materials Research*, 10, 303-310 (1976).